

# Cosmic ray photodisintegration and the knee of the spectrum

Julián Candia, Luis N. Epele and Esteban Roulet

*Phys. Dept., U. of La Plata, CC67, 1900, La Plata, Argentina.*

December 2, 2024

## Abstract

We explore in some detail the scenario proposed to explain the observed knee of the cosmic ray (CR) spectrum as due to the effects of photodisintegration of the CR nuclei by interactions with optical and soft UV photons in the source region. We show that the photon column densities needed to explain the experimental data are significantly lower than those obtained in previous estimations which neglected multinucleon emission in the photodisintegration process. We also treat more accurately the photodisintegration thresholds, we discuss the effects of photopion production processes and the neutron escape mechanism, identifying the physical processes responsible for the qualitative features of the results. This scenario would require the CR nuclei to traverse column densities of  $\sim 5 \times 10^{27} - 2 \times 10^{28}$  eV/cm<sup>2</sup> after being accelerated in order to reproduce the observed knee, and predicts that the CR composition should become lighter above  $\sim 10^{16}$  eV.

## 1 Introduction

It is widely accepted nowadays that cosmic rays (CRs) with energies per particle up to about  $10^{18}$  eV are protons and nuclei of galactic origin. Furthermore, it is well established that the full CR energy spectrum has a power-law behavior with a steepening taking place at the so-called knee, corresponding to an energy  $E_{knee} = 3 \times 10^{15}$  eV. Although it is well known that the CR composition below the knee has a significant heavy component, its behavior beyond the knee remains somewhat controversial. Indeed, above  $10^{14}$  eV/nucleus the information about the CR mass composition has to be drawn from extensive air shower observations at ground level, and the data obtained has to be interpreted assuming a certain hadronic interaction model. Unfortunately, the differences between the hadronic models (e.g. QGSJET,

VENUS, SIBYLL or HDPM) yield significant discrepancies in the final results [1], and this turns out to be even more cumbersome once we compare results coming from different experimental facilities. Thus, the CR mass composition beyond the knee is not definitively established yet, with some observations [2] suggesting that it turns lighter and others claiming that the heavier components become dominant [3].

The attempts made so far to explain the physical origin of the knee of the cosmic ray spectrum can be roughly classified into three kind of models. One of them exploits the possibility that the acceleration mechanisms could be less effective above the knee [4, 5, 6], while a second one assumes that leakage from the Galaxy plays the dominant role in suppressing CRs above the knee [7, 8, 9]. The third scenario, originally proposed by Hillas [10], considers nuclear photodisintegration processes (and proton energy losses by photomeson production), in the presence of a background of optical and soft UV photons in the source region, as the main responsible for the change in the CR spectrum. The first two scenarios are based on a rigidity dependent effect which consequently produces a change in the spectral slope of each nuclear component with charge  $Z$  at an energy  $\sim E_{\text{knee}}Z$ . Hence, it removes first the protons and the lighter nuclei and only at larger energies affects the heavier nuclei, predicting that the CR mass composition should become heavier beyond the knee. On the contrary, the third scenario predicts a lighter CR composition above the knee due to the disintegration of the propagating nuclei. The predictions of this last scenario have been worked out by Karakula and Tkaczyk [11] some years ago. The aim of the present paper is to re-evaluate in detail the propagation of nuclei and protons in the source region following their approach, but taking into account some additional features that turn out to be important for the determination of the source parameters required for the scenario to work. In particular, we re-evaluate the nuclear photodisintegration rates taking into account multinucleon emission processes, we introduce more accurate threshold energies in the giant dipole resonance for every stable nucleus (according to recent remarks by Stecker and Salamon [12]), and discuss the impact of the neutron mechanism [13] which would allow the escape of neutrons from the source without further energy losses. Moreover, we show that by introducing a non negligible lower cutoff to the power-law photon distribution, the abrupt suppression of the all-particle CR spectrum above  $10^{17}$  eV previously obtained [11] is prevented, and hence the underlying reason for that effect is identified. Let us also mention that although we focus our study here on the scenario proposed to explain the observed steepening at the knee, we expect that our general considerations about the treatment of photodisintegration processes should also be relevant in other contexts.

## 2 The propagation of cosmic rays

### 2.1 The source and the photon background spectra

As already mentioned, we deal with a model that considers the propagation of cosmic rays through a background of optical and soft UV photons present around the CR source. If the typical energy of the photons is in the optical range (1 – 10 eV), the photodisintegration of CR nuclei will start to be efficient at CR energies  $E \geq A \times 10^{15}$  eV. This is so because in the CR rest frame the optical photon (which is boosted by a relativistic factor  $\gamma \geq 10^6$ ) appears as an energetic gamma ray with  $E \geq 1 - 10$  MeV, i.e. capable of photodisintegrating the nucleus. We assume that the source emits nuclei with mass number  $A$  (with  $A$  ranging from 1 to 56). Since there is only one stable isotope for a nucleus of a given mass  $A$  along most of the decay chain from  $^{56}\text{Fe}$  to  $^1\text{H}$ , we take for definiteness a unique charge  $Z$  associated to any given value of  $A$ . The differential fluxes emitted by the source are assumed to be given by power-law distributions

$$\phi_i^0(E) = \Phi_i^0 E^{-\gamma_i} \quad (1)$$

(where  $i = 56 - A$  throughout). The intensities  $\Phi_i^0$  and spectral indices  $\gamma_i$  were taken from the detailed knowledge about CR mass composition below the knee (for energies per particle above  $\sim \text{few } Z \times 10^{10}$  eV) [14]. This assumption is reasonable within this scenario, since the mechanisms of energy loss during propagation (i.e. the process of nuclear photodisintegration and the photopion production by protons) show up first at energies above  $\sim 10^{15}$  eV.

For the photon background that surrounds the source we consider that its spectrum follows either a (thermal) Planckian-type distribution given by

$$n(\epsilon) = \frac{\rho}{2\zeta(3)(k_B T)^3} \frac{\epsilon^2}{\exp(\epsilon/k_B T) - 1} \quad (2)$$

where  $k_B$  is the Boltzmann constant,  $T$  the absolute temperature and  $\zeta$  the Riemann zeta function (such that  $\zeta(3) \approx 1.202$ ), or a power-law distribution given by

$$n(\epsilon) = \rho(\alpha - 1) \left( \frac{1}{\epsilon_m^{\alpha-1}} - \frac{1}{\epsilon_M^{\alpha-1}} \right)^{-1} \epsilon^{-\alpha} \quad (3)$$

where  $\epsilon_m$ ,  $\epsilon_M$  are the lower and upper energy cutoffs and  $\alpha$  the assumed spectral index. For both distributions,  $\rho$  represents the total number density and  $n(\epsilon)$  the differential number density corresponding to a photon energy  $\epsilon$ . Defining  $\rho_E$  as the total energy density, one has for the Planckian spectrum

$$\rho_E \approx 2.631 k_B T \rho \quad , \quad (4)$$

while the analogous expression for the power-law spectrum is

$$\rho_E = \frac{\alpha - 1}{2 - \alpha} \left( \epsilon_M^{2-\alpha} - \epsilon_m^{2-\alpha} \right) \left( \frac{1}{\epsilon_m^{\alpha-1}} - \frac{1}{\epsilon_M^{\alpha-1}} \right)^{-1} \rho . \quad (5)$$

We adopt  $\alpha = 1.3$  as in ref. [11], but the introduction of a non negligible lower cutoff  $\epsilon_m$  in the power-law spectrum excludes the presence of an abundant number of low energy (infrared) photons that would otherwise play the dominant role in the photodisintegration above  $10^{17}$  eV, as was the case in ref. [11].

## 2.2 Propagation of nuclei: photodisintegration

The main mechanism of energy loss for nuclei with energy per particle below  $10^{18}$  eV propagating through these photon backgrounds is the process of photodisintegration. In fact, a nucleus of mass  $A = 56 - i$  and Lorentz factor  $\gamma = E/Am_pc^2$  that propagates through a photon distribution  $n(\epsilon)$  (as, for example, those of eqs. (2) and (3)) has a rate of emission of  $j$  nucleons given by

$$R_{ij}(E) = \frac{1}{2\gamma^2} \int_{\epsilon'_{thr,ij}/2\gamma}^{\infty} d\epsilon \frac{n(\epsilon)}{\epsilon^2} \int_{\epsilon'_{thr,ij}}^{2\gamma\epsilon} d\epsilon' \epsilon' \sigma_{ij}(\epsilon'), \quad (6)$$

where  $\sigma_{ij}$  is the corresponding photodisintegration cross section,  $\epsilon$  the photon energy in the observer's system and  $\epsilon'$  its energy in the rest frame of the nucleus. In order to calculate  $R_{ij}$  we fitted  $\sigma_{ij}$  with the parameters given in Tables I and II of ref. [15], while the reaction thresholds  $\epsilon'_{thr,ij}$  were taken from Table I of ref. [12]. A useful quantity to take into account all reaction channels is the effective emission rate given by

$$R_{i,eff} = \sum_{j \geq 1} j R_{ij} . \quad (7)$$

At low energies ( $\epsilon'_{thr,ij} \leq \epsilon' \leq 30$  MeV), the cross section  $\sigma_{ij}(\epsilon')$  is dominated by the giant dipole resonance and the photodisintegration proceeds chiefly by the emission of one or two nucleons. Note that, according to recent remarks pointed out in ref. [12], we employ threshold energies that depend both on the nucleus and on the number of emitted nucleons. The improvement consists in shifting the threshold energy, that was previously assumed to be  $\epsilon'_{thr} = 2$  MeV for all reaction channels and all nuclei [11, 15], to higher energies, such that single-nucleon emission has now a typical threshold of  $\sim 10$  MeV, while the double-nucleon emission energy threshold becomes typically  $\sim 20$  MeV. Although the appearance of the knee in this scenario is ultimately a threshold effect, the improved calculation including the change in the specific threshold energies has however a minor impact on the resulting

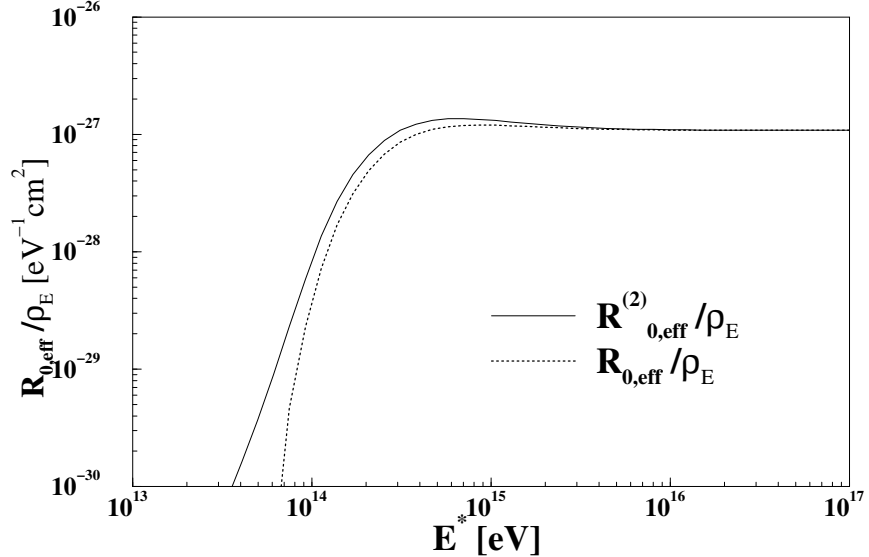


Figure 1: Plots of  $R_{0,eff}/\rho_E$  versus energy per nucleon  $E^*$  for a thermal photon spectrum (with  $k_B T = 10$  eV).  $R_{0,eff}^{(2)}$  was evaluated using the fixed threshold energy  $\epsilon_m = 2$  MeV, while  $R_{0,eff}$  corresponds to the improved threshold energies according to ref. [12].

emission rates when compared with those obtained with a fixed threshold energy  $\epsilon'_{thr} = 2$  MeV. This can be appreciated in Figure 1, where plots of  $R_{i,eff}/\rho_E$  vs energy per nucleon  $E^*$  are shown for a  $^{56}\text{Fe}$  nucleus ( $i = 0$ ) propagating through a thermal photon spectrum (with  $k_B T = 10$  eV). The emission rate  $R_{0,eff}$  (calculated with the specific threshold energies) shows a small shift towards higher energies with respect to that obtained by means of the fixed threshold energy (labeled  $R_{0,eff}^{(2)}$ ). The reason for this reduced effect of the threshold shifts is that the dominant photodisintegration effects are due anyhow to the energies around the giant resonance peak, which for single-nucleon emission are typically peaked around  $\sim 20$  MeV and for double-nucleon emission around  $\sim 26$  MeV, and hence clearly well above the threshold energies.

At higher energies,  $\sigma_{ij}(\epsilon')$  is approximately flat and the multinucleon emission acquires a higher probability, becoming actually dominant for heavy nuclei, for which the probability for single nucleon emission is of only 10%. To estimate the relevance of multinucleon emission processes, we compare the effective rate from eqs. (6) and (7) with the emission rate that neglects multinucleon processes (as calculated in ref. [11]). Figure 2(a) shows plots of  $R_{i,eff}/\rho_E$  versus energy per nucleon  $E^*$  for a  $^{56}\text{Fe}$  nucleus ( $i = 0$ ) propagating through a thermal photon spectrum (with  $k_B T = 1.8$  eV). From the figure it becomes evident that multinucleon processes play an

important role, increasing the emission rate at high energies by a factor of  $\sim 4$  with respect to the single nucleon emission results. Analogously, Figure 2(b) shows the corresponding plots for a power-law photon spectrum with upper energy cutoff  $\epsilon_M = 20$  eV and spectral index  $\alpha = 1.3$ . From this figure we can also see the effect of introducing a non negligible lower cutoff in the spectrum. In fact, we observe that with a negligible cutoff (e.g.  $\epsilon_m = 10^{-6}$  eV) the emission rate grows steadily, because increasingly abundant low energy (infrared) photons give in this case the dominant contribution to the rates. They also keep the influence of the giant resonance dominant even at high particle energies, and hence in this case the multinucleon emission has little impact. However, if we take a non negligible cutoff into account (for instance,  $\epsilon_m = 0.8$  eV), we find that the flat high energy regime of  $\sigma_i$  now dominates beyond a given value of  $E^*$  and hence the emission rate saturates at high energies. Comparing the two emission rate curves with non negligible cutoff, we observe again that multinucleon emission processes lead to a significant increase (by the same factor of  $\sim 4$  we already encountered) in the emission rate. Thus, introducing a non negligible lower cutoff energy in the power-law photon spectrum the results should not differ much from those with the thermal photon spectrum and, being the rates with multinucleon emission larger, they should also require smaller photon densities than those previously estimated in ref. [11] to produce similar overall effects.

It should be noticed that in Figures 1 and 2 we have chosen to plot the emission rates as functions of the energy per nucleon  $E^*$ , instead of energy per nucleus  $E$ , because it is  $E^*$  that remains constant during photodisintegration and also because for different nuclei the shapes of the cross section are similar with the maxima occurring approximately at the same values of  $E^*$ .

The appropriate diffusion equations that describe the propagation of nuclei are:

$$\frac{\partial \phi_i(E^*, x)}{\partial x} = -\phi_i(E^*, x) \sum_{j \geq 1} R_{ij}(E^*) + (1 - \delta_{0i}) \sum_{j=1}^i R_{(i-j)j}(E^*) \phi_{i-j}(E^*, x), \quad (8)$$

where  $\phi_i(E^*, x)$  is the differential flux of a nucleus of mass  $A = 56 - i$  (for  $0 \leq i \leq 54$ ) with an energy per nucleon  $E^*$  at propagation distance  $x$  from the source,  $R_{ij}(E^*)$  is the above defined emission rate and  $\delta_{ij}$  is the Kronecker delta. The exact solution of these equations (i.e., the differential fluxes at propagation distance  $L$ ) is given by:

$$\phi_i(E^*, L) = \sum_{j=0}^i b_{ij}(E^*) \exp\left(-\sum_{k \geq 1} R_{jk}(E^*) L\right), \quad (9)$$

where

$$b_{ii} = \phi_i^0(E^*) - (1 - \delta_{0i}) \sum_{j=0}^{i-1} b_{ij}(E^*) \quad (10)$$

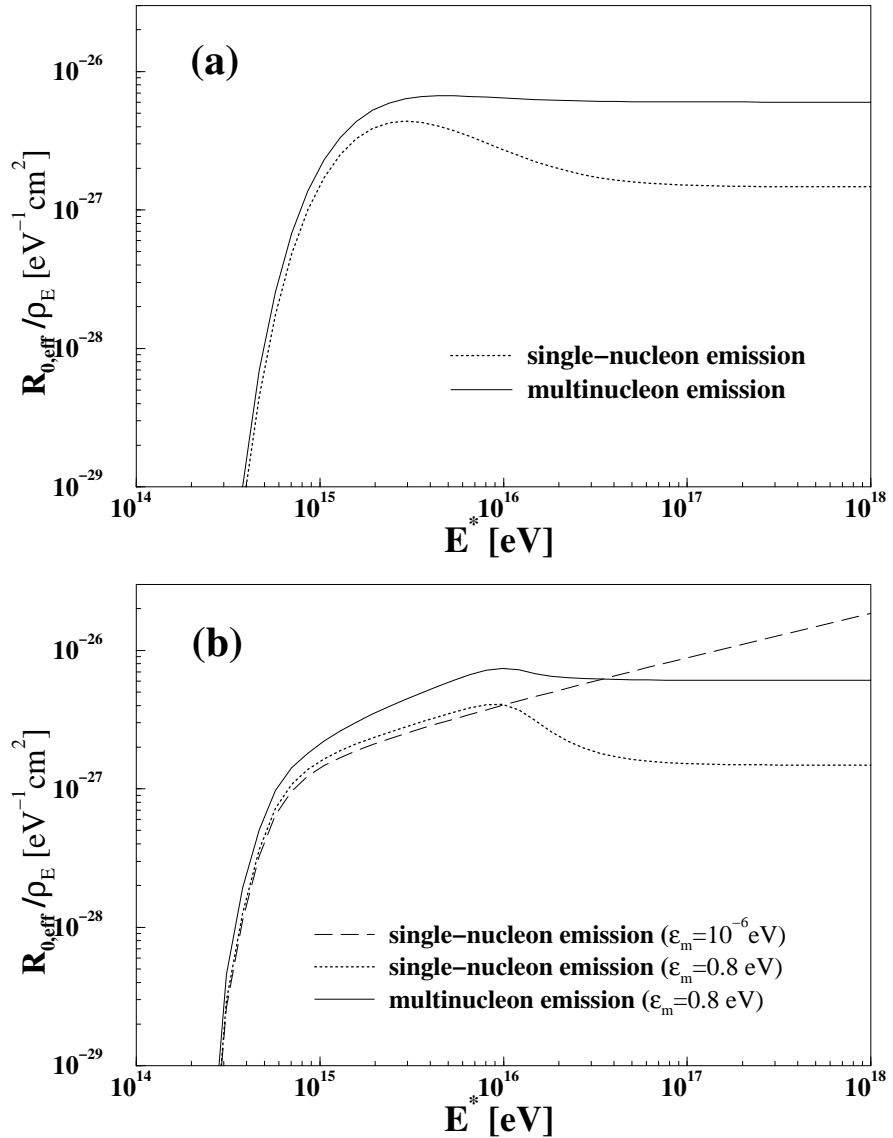


Figure 2: Plots of  $R_{0,eff}/\rho_E$  versus energy per nucleon  $E^*$ . (a) Results for a thermal photon spectrum with  $k_B T = 1.8$  eV. (b) Results for a power-law photon spectrum with upper energy cutoff  $\epsilon_M = 20$  eV and spectral index  $\alpha = 1.3$ . The multinucleon emission rate corresponds to a lower energy cutoff  $\epsilon_m = 0.8$  eV, while the single-nucleon emission rates correspond to  $\epsilon_m = 10^{-6}, 0.8$  eV, as indicated.

and

$$b_{ij} = \frac{\sum_{k=1}^{i-j} b_{(i-k)j}(E^*) R_{(i-k)k}(E^*)}{\sum_{k \geq 1} R_{ik}(E^*) - \sum_{k \geq 1} R_{jk}(E^*)}, \quad \text{for } i > j. \quad (11)$$

Recalling that the emission rates  $R_{ij}$  are linear in the photon energy density  $\rho_E$ , it should be noted that, as expected, the fluxes only depend on the column density  $\rho_E L$ . It also should be pointed out that, since the diffusion equations only depend on the energies per nucleon  $E^*$ , the final CR spectra require the re-calculation of the solution (eqs.(9)-(11)) in terms of energy per nucleus.

### 2.3 Propagation of protons

The main energy loss mechanism that must be taken into account for the propagation of protons is the photomeson production process. We have to distinguish between the primary protons produced at the source with an initial flux  $\phi_{i=55}^0$  (as given by eq.(1)) and the nucleons released as by-products of the nuclear photodisintegration. The fluxes corresponding to these (secondary) protons and neutrons ( $\phi^{sp}$  and  $\phi^n$ , respectively) can be easily determined from the solution for the nuclear fluxes, as we will see in the following. Let  $\phi_i^N(E, x)$  be the differential flux of nucleons of energy  $E$  produced within a distance  $x$  away from the source by the photodisintegration of nuclei of mass number  $A = 56 - i$  and energy per nucleon  $E^* = E/A$ . Then, the equation governing the evolution of the fluxes is

$$\frac{\partial \phi_i^N(E, x)}{\partial x} = \phi_i(E^*, x) \sum_{j \geq 1} j R_{i,j}(E^*) , \quad \text{for } 0 \leq i \leq 54 , \quad (12)$$

(with the initial condition  $\phi_i^N(E, x = 0) = 0$ ) and its solution reads

$$\phi_i^N(E, L) = \sum_{j=0}^i \left( \frac{\sum_{k \geq 1} k R_{ik}(E^*)}{\sum_{k \geq 1} R_{jk}(E^*)} \right) b_{ij}(E^*) \left[ 1 - \exp \left( - \sum_{k \geq 1} R_{jk}(E^*) L \right) \right] . \quad (13)$$

Thus, the total fluxes of secondary protons and neutrons are found by performing the weighted sums over index  $i$ :

$$\phi^{sp}(E, L) = \sum_{i=0}^{54} \frac{Z_i}{56 - i} \phi_i^N(E, L) , \quad (14)$$

$$\phi^n(E, L) = \sum_{i=0}^{54} \left( 1 - \frac{Z_i}{56 - i} \right) \phi_i^N(E, L) , \quad (15)$$

where  $Z_i$  is the charge of the  $i$ -nucleus.

We will also discuss the possible impact of the so-called neutron mechanism[13], which could take place in the presence of a magnetic field in the source region. Indeed, a magnetic field would retain the charged particles within that region for some period of time, while non-charged particles would be able to escape rapidly. In that case, we will consider that the flux of neutrons  $\phi^n$  adds to the final all-particle CR flux neglecting any energy losses, while the flux of secondary protons  $\phi^{sp}$ , combined with the initial flux of primary protons  $\phi_{i=55}^0$ , will undergo energy losses due to the well studied process of photopion production. Indeed, since a background photon looks like a high-energy gamma ray in the proton rest frame, the photopion reactions



proceed with a reaction rate given by

$$g(E) = \frac{1}{2\gamma^2} \int_{\epsilon'_{thr}/2\gamma}^{\infty} d\epsilon \frac{n(\epsilon)}{\epsilon^2} \int_{\epsilon'_{thr}}^{2\gamma\epsilon} d\epsilon' \epsilon' \sigma_{\gamma p}(\epsilon') K(\epsilon'), \quad (18)$$

where, analogously to eq. (6),  $\gamma = E/m_p c^2$  is the Lorentz factor of the proton,  $\sigma_{\gamma p}$  is the  $\gamma p$  interaction cross section (parametrized from experimental data compiled in ref.[16]),  $K$  is the coefficient of inelasticity (defined as the average relative energy loss of the proton),  $\epsilon$  the photon energy in the observer's system and  $\epsilon'$  its energy in the rest frame of the proton. The energy threshold for photopion production is  $\epsilon'_{thr} = 145$  MeV.

Then, if we call  $\phi^p(E, x)$  and  $\phi^{*n}(E, x)$  the differential fluxes of protons and neutrons of energy  $E$  (produced by the reactions given by eqs.(16) and (17), respectively) after propagating a distance  $x$  from the source, the corresponding diffusion equations are

$$\frac{\partial \phi^p(E, x)}{\partial x} = -g(E)\phi^p(E, x) + \frac{1}{2} \frac{1}{(1-K)} g\left(\frac{E}{1-K}\right) \phi^p\left(\frac{E}{1-K}, x\right) \quad (19)$$

and (neglecting neutron energy losses)

$$\frac{\partial \phi^{*n}(E, x)}{\partial x} = \frac{1}{2} \frac{1}{(1-K)} g\left(\frac{E}{1-K}\right) \phi^p\left(\frac{E}{1-K}, x\right), \quad (20)$$

where the factors  $\frac{1}{2}$  arise from the relative probability of occurrence of reactions (16) and (17). The coefficient of inelasticity  $K$  was given a typical value  $K = 0.3$ , irrespective of proton energy [11]. The initial conditions to solve these differential equations are

$$\phi^p(E, x = 0) = \phi_{i=55}^0(E) + \phi^{sp}(E, L) \quad (21)$$

and

$$\phi^{*n}(E, x = 0) = 0 , \quad (22)$$

respectively. In the first one we assumed for simplicity that the secondary protons produced by photodisintegration of nuclei add directly to the initial proton spectrum. This is justified since whenever the photopion processes are relevant, the photodisintegration is very efficient and hence nuclei are rapidly disintegrated. The solution to eq.(19) turns out to be

$$\phi^p(E, L) = \sum_{l=0}^{\infty} \phi_l^p(E, L) , \quad (23)$$

where

$$\phi_0^p(E, L) = \phi^p(E, 0) \exp(-g(E)L) , \quad (24)$$

while for  $l > 0$

$$\phi_l^p(E, L) = \frac{\phi^p\left(\frac{E}{(1-K)^l}, 0\right)}{(2(1-K))^l} \prod_{j=1}^l g\left(\frac{E}{(1-K)^j}\right) \sum_{n=0}^l \frac{\exp\left(-g\left(\frac{E}{(1-K)^n}\right)L\right)}{\prod_{\substack{m=0 \\ m \neq n}}^l \left[g\left(\frac{E}{(1-K)^m}\right) - g\left(\frac{E}{(1-K)^n}\right)\right]} . \quad (25)$$

For the neutron component, the solution to eq.(20) reads

$$\phi^{*n}(E, x) = \sum_{l=0}^{\infty} \phi_l^{*n}(E, x) , \quad (26)$$

where

$$\phi_0^{*n}(E, L) = \frac{\phi^p\left(\frac{E}{1-K}, 0\right)}{2(1-K)} \left(1 - \exp\left(-g\left(\frac{E}{1-K}\right)L\right)\right) , \quad (27)$$

while for  $l > 0$

$$\begin{aligned} \phi_l^{*n}(E, L) = & \frac{\phi^p\left(\frac{E}{(1-K)^{l+1}}, 0\right)}{(2(1-K))^{l+1}} \prod_{j=0}^l g\left(\frac{E}{(1-K)^{j+1}}\right) \times \\ & \sum_{n=0}^l \frac{1 - \exp\left(-g\left(\frac{E}{(1-K)^{n+1}}\right)L\right)}{g\left(\frac{E}{(1-K)^{n+1}}\right) \prod_{\substack{m=0 \\ m \neq n}}^l \left[g\left(\frac{E}{(1-K)^{m+1}}\right) - g\left(\frac{E}{(1-K)^{n+1}}\right)\right]} . \end{aligned} \quad (28)$$

The linearity of the photopion reaction rate  $g(E)$  with respect to the photon energy density  $\rho_E$  (as implied by eq.(18)) causes the proton and neutron fluxes to depend only on the column density  $\rho_E L$ , similarly as for the fluxes of nuclei.

### 3 Results and comparison with observations

So far, we wrote down the appropriate diffusion equations governing the propagation of CR particles, and we found their exact solutions: eqs.(9)-(11) for nuclei, eqs.(13),(15) and (26)-(28) for neutrons (that eventually decay into protons outside the source region), and eqs.(23)-(25) for protons (that undergo energy losses due to photopion production), the sum of all these contributions being the total CR flux  $\phi_{total}$ . We can now investigate how  $\phi_{total}$  depends on the assumed photon distributions around the source, namely on the column density  $\rho_E L$  and on the parameters involved in the photon spectral distributions (eqs.(2) and (3)).

Figure 3(a) shows the total CR differential flux as a function of the energy per particle for a Planckian spectrum with  $k_B T = 1.8$  eV and several values for the column density  $\rho_E L$ . Analogously, Figure 3(b) shows the results corresponding to a Planckian spectrum with  $k_B T = 10$  eV. To compare our results with experimental data, the figures also show the observed spectra measured by different experiments (CASABLANCA, DICE, Tibet, PROTON satellite and AKENO) [1, 2, 17].

The effect of increasing the temperature is clearly that of shifting the knee towards lower energies, while the effect of increasing  $\rho_E L$  is that of intensifying the steepening at the knee. This behavior is easily explained by the fact that it is the nuclear photodisintegration the responsible for the occurrence of the knee (since photopion production processes show up at higher energies). Then, if the photon temperature (and thus, the mean photon energy) is larger, the particle energy required for the nuclei to disintegrate decreases. Furthermore, CR propagation cannot be affected by  $\rho_E L$  below the knee, where the photodisintegration has not set up yet, but above the knee the disintegration rates have a linear dependence on  $\rho_E$ . Hence, we should expect  $\rho_E L$  to control the steepening in the knee region, in agreement with the results shown in the figures. In ref. [11] the best fit to observations for the Planckian spectrum was that corresponding to  $k_B T = 1.8$  eV and  $\rho_E L = 2.25 \times 10^{29}$  eV/cm<sup>2</sup>. For the sake of comparison, Figure 3(a) shows our results for the same temperature. It is clearly observed that the new results are compatible with experimental data for column density values as low as  $\rho_E L = 5 \times 10^{27}$  eV/cm<sup>2</sup>, i.e. up to  $\sim 50$  times lower than the previous result. Figure 3(b) shows that the corresponding results for  $k_B T = 10$  eV fit well to observations for column densities in the range  $\rho_E L = 5 \times 10^{27} - 2 \times 10^{28}$  eV/cm<sup>2</sup>.

Figures 4(a) and 4(b) show plots of mean mass composition  $\langle \ln A \rangle$  versus  $E$  corresponding to the Planckian photon spectra with  $k_B T = 1.8$  eV and  $k_B T = 10$  eV, respectively. For comparison, we also show the CR mass composition measured by different experiments [1, 2, 18]. One can observe that solutions corresponding to the largest plotted values of column density  $\rho_E L$  imply that CRs above the knee are chiefly constituted by protons, in disagreement with experimental data; the non-negligible contribution of heavier CR components beyond the knee imposes an

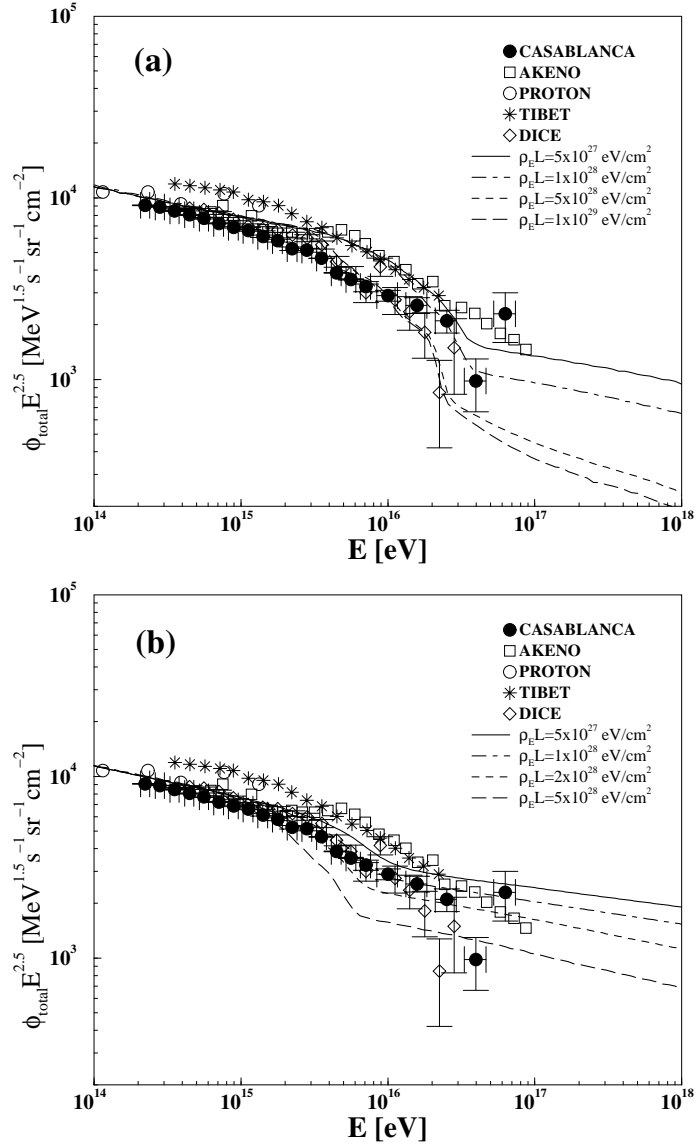


Figure 3: Plots showing the total CR flux versus the energy per particle for thermal spectra with (a)  $k_B T = 1.8$  eV and (b)  $k_B T = 10$  eV, and several values for the column density  $\rho_E L$ , as indicated. For the sake of comparison, experimental data measured by different experiments are also shown.

upper limit on the column density around  $(\rho_E L)_{max} \approx 2 \times 10^{28} \text{ eV/cm}^2$ . This result stresses again the fact that multinucleon emission processes play a significant role in CR propagation within this scenario. We also see that, although the solutions with lower column density ( $\rho_E L \leq (\rho_E L)_{max}$ ) fit well to some data sets within error bars, the composition beyond the knee seems to be somewhat suppressed. Nevertheless, we should bear in mind that we have employed just one source with a fixed column density, and that in a realistic situation there would be many sources, each with a different environment of radiation. Avoiding any detailed calculations, we may think about the contribution of one additional source. If it happens to have a column density  $\rho_E L$  somewhat smaller, it would lead to a flatter flux; then, whereas the first source would be responsible for the occurrence of the knee, the second one would keep a non-vanishing nuclear component beyond the knee. Furthermore, in the computations we assumed that all nuclei traverse the same distance  $L$ , thus disregarding the fact that the magnetic field present in the source region should retain more effectively the heavier nuclei at any given CR energy. Taking this into account (for instance, assuming that a nucleus traverses a distance in the photon background proportional to its charge) we would find that, while the disintegration would be very effective for heavy nuclei (and would be, in fact, responsible for forming the knee), it would be less effective for the lighter nuclei (since the column density for them would be much smaller) and they could then survive beyond the knee. Hence, we see that this scenario can easily account for a change in the composition towards lighter nuclei above the knee, which is apparent in some of the existing data. On the contrary, rigidity dependent scenarios predict the opposite trend, and may have difficulties to account for some measurements. It has indeed been pointed out that they would require the introduction of an ad-hoc additional light component above the knee to reproduce the observations [19].

The results for the power-law photon spectrum (with a lower cutoff energy in the infrared range) should not differ much from the ones obtained for the Planckian spectrum, and this behavior was in fact corroborated. We shall then here merely discuss the dependence of the results on the lower cutoff energy. Let us fix the spectral index and the upper cutoff energy at the values found in ref. [11] to correspond to the best fit to experimental data, namely  $\alpha = 1.3$  and  $\epsilon_M = 20 \text{ eV}$ . Figure 5 shows  $\phi_{total}$  versus  $E$  for power-law distributions with column density  $\rho_E L = 10^{28} \text{ eV/cm}^2$  and several values for the lower cutoff energy ( $\epsilon_m = 0.01, 0.1, 0.8 \text{ eV}$ ). It is found that, apart from minor differences arising from spectrum normalization, lower values of  $\epsilon_m$  yield lower fluxes in the high energy end. The explanation for this is that from the expression for the photodisintegration emission rate (eq.(6)) it turns out that the role of  $\epsilon_m$  is that of determining a value of the particle energy  $E$ , such that below  $E$  the giant dipole resonance dominates, while above  $E$  the flat high energy regime of  $\sigma$  prevails. As we lower  $\epsilon_m$ , more photons with lower energy become available so that the flux suppression imposed by the giant resonance extends to higher particle

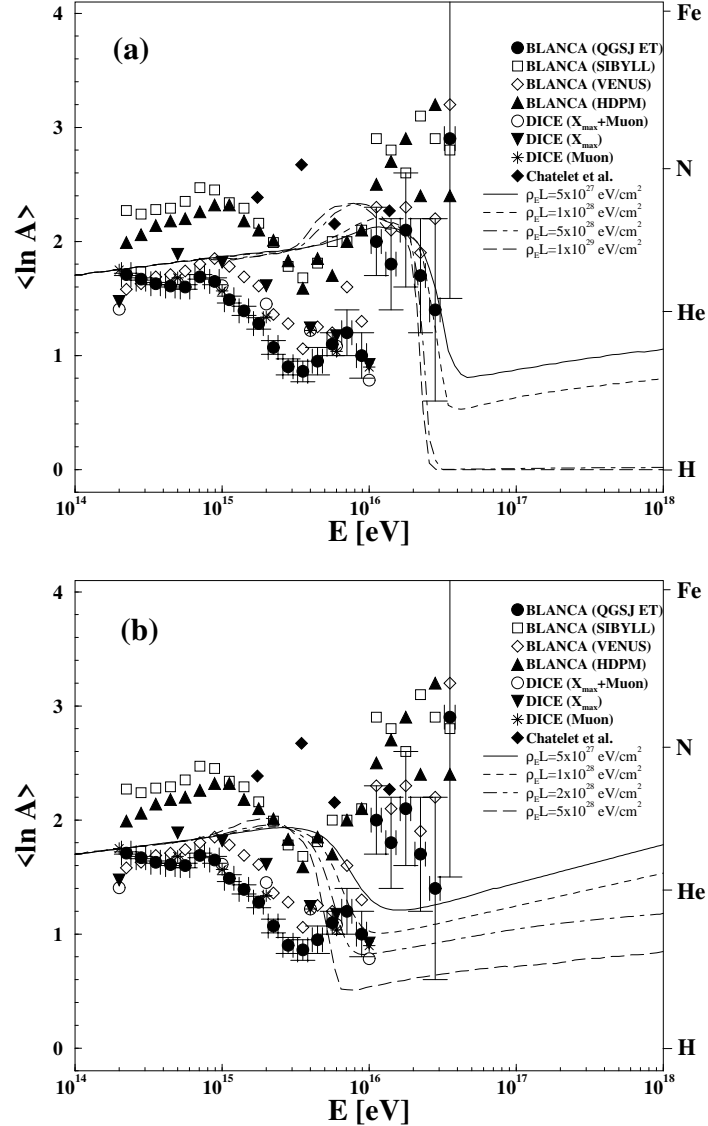


Figure 4: Plots of mean mass composition  $\langle \ln A \rangle$  versus  $E$  corresponding to the Planckian photon spectra with (a)  $k_B T = 1.8$  eV and (b)  $k_B T = 10$  eV. For comparison, the CR mass composition measured by different experiments is also shown. Notice that several data sets exhibit the same qualitative behavior, since they correspond to the same experimental data and differ only in the hadronic models used to interpret the observations.

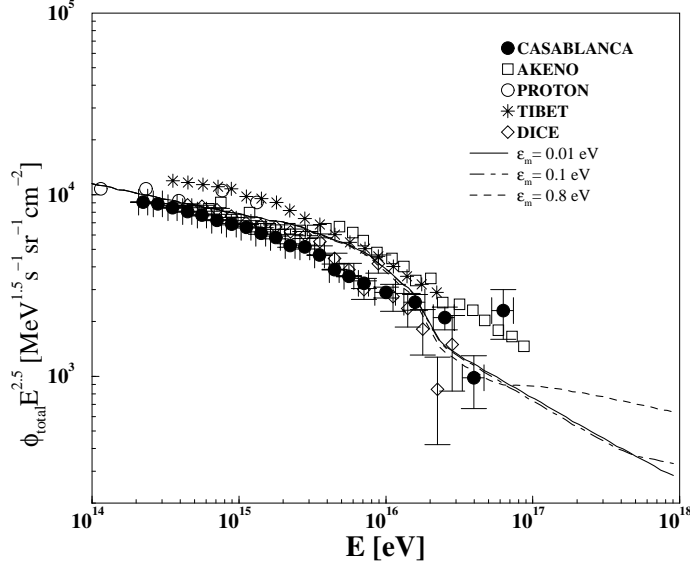


Figure 5: Plots showing the total CR flux versus the energy per particle for power-law spectra with  $\alpha = 1.3$ ,  $\epsilon_M = 20 \text{ eV}$ ,  $\rho_{EL} = 10^{28} \text{ eV/cm}^2$  and several values for the lower cutoff energy ( $\epsilon_m = 0.01, 0.1, 0.8 \text{ eV}$ ). For comparison, experimental data measured by different experiments are also shown.

energies.

This analysis provides a suitable explanation of the results shown in Figure 5, as well as those of Figure 2(b). The results previously obtained for power-law spectra [11] show an extremely abrupt flux suppression that seems to be in contrast with experimental data (CR energy spectra and, especially, CR mass composition) above  $E = 10^{17} \text{ eV}$ , and can be attributed to the negligible value for  $\epsilon_m$  adopted there. The use of a non negligible cutoff prevents the flux suppression and provides a better fit to observations in this energy region. It should also be remarked that a solution yielding an excessive CR flux at energies above  $10^{17} \text{ eV}$  is by no means troublesome since it is clear that at these high energies efficient leakage of CRs from the Galaxy cannot be disregarded, and that a less effective acceleration could also be playing a role. These mechanisms would clearly contribute to lower the CR flux, so that it does not seem reasonable to expect a reliable explanation of the CR spectrum by photodisintegration processes alone beyond  $E \sim 10^{17} \text{ eV}$ .

Figure 6 shows plots of the proton and neutron components ( $\phi^p + \phi^{sp}$  and  $\phi^n + \phi^{*n}$ , respectively) as well as the total CR flux  $\phi_{\text{total}}$  for the Planckian photon spectrum with  $k_B T = 1.8 \text{ eV}$  and  $\rho_{EL} = 2 \times 10^{29} \text{ eV/cm}^2$ . In order to estimate the possible effects of the neutron mechanism, we also plotted the total CR flux that is obtained ignoring the escape of neutrons, labeled  $\phi_{\text{total}}^*$ . From the figure it is seen that the neutron mechanism raises the CR total flux by  $\sim 100\%$  for  $E \geq 5 \times 10^{16} \text{ eV}$ .

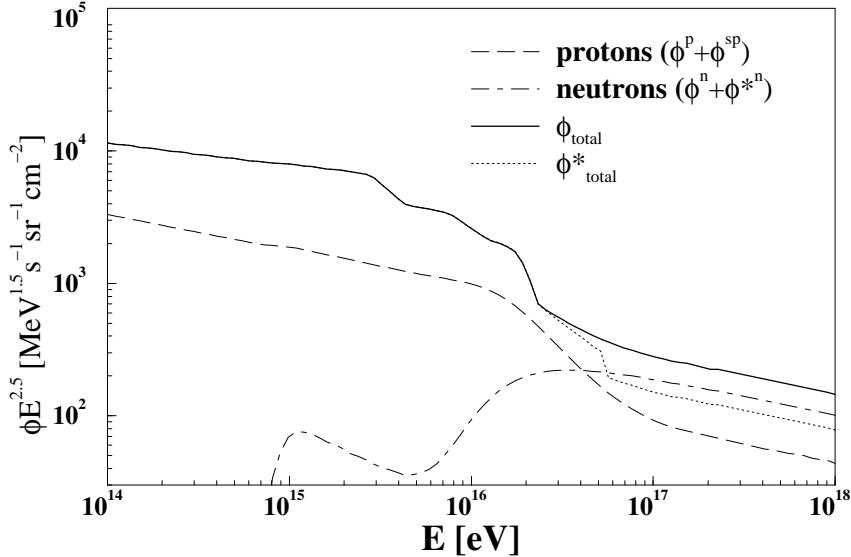


Figure 6: Plots showing the proton flux ( $\phi^p + \phi^{sp}$ ), the neutron flux ( $\phi^n + \phi^{*n}$ ) and the total CR flux ( $\phi_{total}$ ) versus the energy per particle for a thermal photon spectrum with  $k_B T = 1.8$  eV and  $\rho_E L = 2 \times 10^{29}$  eV/cm<sup>2</sup>. Also shown is the total CR flux ( $\phi_{total}^*$ ) that is obtained ignoring the escape of neutrons.

If we adopted a column density  $\rho_E L = 10^{29}$  eV/cm<sup>2</sup>, the corresponding flux increment would be only  $\sim 10\%$ . Nevertheless, it should be noted that these results correspond to very high column densities (actually inconsistent with the observed CR composition), and that effects arising from the neutron escape mechanism turn out to be negligible for lower values of the column density  $\rho_E L$ , for which also the photopion losses of protons can be altogether ignored.

As a summary, we have considered in more detail the photodisintegration of CR nuclei in the scenario in which their interaction with optical and soft UV photons around the source is responsible for the steepening of the spectrum and for the change in composition above the knee. The more accurate treatment of the nuclear processes, in particular the inclusion of the multinucleon emission, implies that the required photon column densities are lower (by an order of magnitude) than previously obtained. Although we have not discussed the nature of the photon background around the source, the necessary photon column densities favor sources which are rather compact [11], such as pulsars. The main difference between this scenario and other (rigidity dependent) explanations proposed for the knee is the resulting CR composition, which here becomes lighter above  $\sim 10^{16}$  eV.

## Acknowledgments

Work supported by CONICET, ANPCyT and Fundación Antorchas, Argentina. E. R. thanks A. Dar for fruitful discussions on the subject.

## References

- [1] J.W. Fowler et al., astro-ph/0003190.
- [2] S.P. Swordy and D.B. Kieda, *Astropart. Phys.* **13** (2000), 137.
- [3] M. Amenomori et al. (Mt Fuji Emulsion Chamber Collaboration), in: *Proc. 19th Int. Cosmic Ray Conf.*, La Jolla (1985) Vol.2, p.206-208.
- [4] C.E. Fichtel and J. Linsley, *ApJ* **300** (1986), 474.
- [5] J.R. Jokipii and G.E. Morfill, *ApJ* **312** (1986), 170.
- [6] K. Kobayakawa et al., astro-ph/0008209.
- [7] S.I. Syrovatsky, *Comm. Astrophys. Space Phys.* **3** (1971), 155.
- [8] J. Wdowczyk and A.W. Wolfendale, *J. Phys. G.* **10** (1984), 1453.
- [9] V.S. Ptuskin et al., *Astron. Astrophys.* **268** (1993), 726-735.
- [10] A.M. Hillas, in: *Proc. 16th Int. Cosmic Ray Conf.*, Kyoto (1979) Vol.8, p.7.
- [11] S. Karakula and W. Tkaczyk, *Astropart. Phys.* **1** (1993), 229.
- [12] F.W. Stecker and M.H. Salamon, *ApJ* **512** (1999), 521.
- [13] V.S. Berezinsky, in: *Proc. Int. Conf. Neutrino-77* (Elbrus), vol.1, p.177 (Nauka, Moscow, 1978).
- [14] B. Wiebel-Sooth et al., *Astron. and Astrophys.* **330** (1998), 389.
- [15] J.L. Puget et al., *ApJ* **205** (1976), 638.
- [16] *Rev. of Part. Phys.*, *Eur. Phys. Jour. C* **15** (2000).
- [17] M. Amenomori et al., *ApJ* **461** (1996), 408.
- [18] E. Chatelet et al., in: *Proc. 22nd Int. Cosmic Ray Conf.*, Dublin (1991) Vol.2, p.45.
- [19] S.V. Ter-Antonyan and L.S. Haroyan, hep-ex/0003006.